Int. J. of GEOMATE, June, 2014, Vol. 6, No. 2 (Sl. No. 12), pp. 919-926
Geotech., Const. Mat. & Env., ISSN:2186-2982(P), 2186-2990(O), Japan

STABILITY ANALYSIS OF AN EARTH DAM FOUNDATION IN TUNISIA

El Ouni Mohamed Ridha[1], Guettaya Ikram[2]

[1,2]National Agronomic Institute of Tunisia, Carthage University, Tunisia

ABSTRACT: Soil liquefaction has been the cause of most geotechnical hazards during earthquake events. Its assessment is an important design consideration for structures made on sandy deposits and situated in seismically active regions. The present paper focuses on the analysis of soil liquefaction potential beneath an earth dam in Tunisia using in situ and laboratory tests results. In order to precise the need of a planned construction, site characterization was carried out with in situ tests (CPT) performed at the dam site before and after vibrocompaction technique. In situ - based simplified procedures have been applied using the data collected before and after the soil densification and the results are so analyzed. Furthermore, the laboratory study includes cyclic triaxial testing of samples retrieved at different densities, confining stresses and cyclic stress ratios and the results were discussed. The obtained results showed a general agreement between the two types of approaches.

Keywords: Liquefaction, In Situ Test, Vibrocompaction, Field Case Histories, Triaxial Tests

1. INTRODUCTION

The prediction of liquefaction and resulting displacements is a major concern for earth structures located in regions of moderate to high seismicity. For instance, the stability of dams during earthquakes must be thoroughly researched since large displacements could lead to overtopping and sudden release of the reservoir and then threat the life and property of residents downstream.

Two basic approaches are available to analyze liquefaction potential triggering using in situ and laboratory tests results.

This paper attempts to present the results of both field (CPT) and laboratory tests that have been used to assess the liquefaction potential of an earth dam foundation in Tunisia. The vibrocompaction technique was selected as the appropriate improvement method against the liquefaction hazard beneath the dam foundation**.**

2. SITE OF PROJECT DAM

Sidi El Barrak earth dam is situated in the extreme North Western coast of Tunisia (figure 1). The site of dam is located at 6.5 km from the Mediterranean Sea, 15 km from the Nefza region and 20 km from the North East of Tabarka city. Total area of the watershed is about 896 km2 and the reservoir level is equivalent to 29 m height. The total capacity of the reservoir is about 275 Million cubic meters. The Sidi El Barrak dam provides irrigation water for fertile lands that extend over an area of 4000 hectares. The heterogenous foundation of dam is predominantly composed by sandy formations. The latter of Quaternaries, Neogene's and Paleogene age consist in alluvial sand and eolian dunes. The rigid stratum level is composed by marls which are apparent at the right side (figure 2).

Fig. 1 Location and Components of dam

According to the Tunisian Central Bureau, ground motions recorded in the western north of Tunisia are characterized by a maximum peak ground Acceleration equal to 0.15g and variable intensities of VII to VIII.

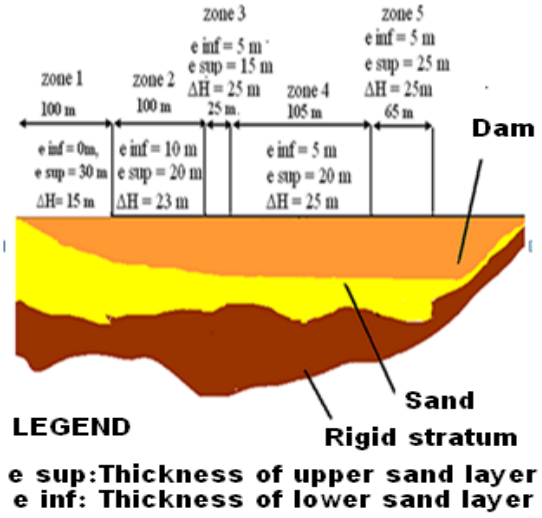

Fig. 2 Geological section of the dam site

In addition, two wells were executed respectively in the left side and in the bed river of Sidi El Barrak dam for samples laboratory testing. Figure 3a and b presents the typical grain size envelopes for depths where the two wells are performed. The results show the sands to be graded from coarse to medium to fine. The uniformity coefficient varies between 2.37 and 7.5 in the left bank and between 2 and 13.6 in the bed river. The median diameter (D50) varies from 0.14 mm to 1.3 mm in the former zone while it varies from 0.13 to 1.4 mm in the latter zone.

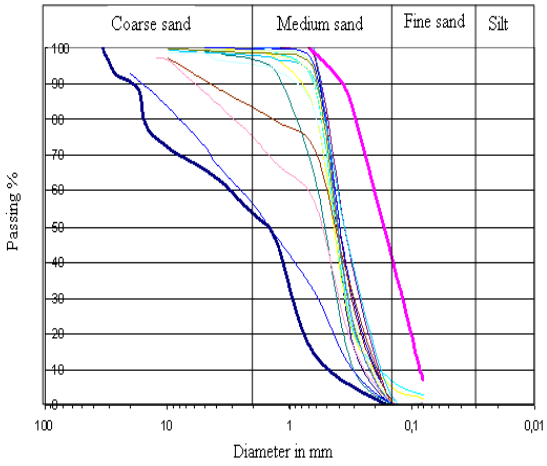

Fig. 3a Grain-size distribution of soil in the left bank

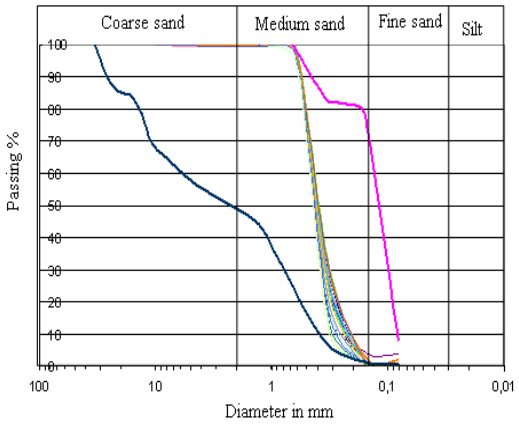

Fig. 3b Grain-size distribution of soil in the river bed

Liquefaction criteria were derived from several case historic studies. Such criteria provided a basis for partitioning the soils vulnerable to severe strength loss as a result of an earthquake shaking. According to the laboratory test results, it is clear that the liquefaction conditions of a sandy soil are met. Indeed, a determination of the soil characteristics using the fig. 3 shows that the median diameter D50 is in the range of 0.05 mm to 1.5 mm and the uniformity coefficient is less than 15. Therefore, there is liquefaction potential in the Sidi El Barrak dam foundation.

Thus, vibrocompaction technique was deemed as the most effective and economical choice in order to obtain a minimum target relative density of 70%, to achieve low static settlements and ensure liquefaction resistance. The treatment of Sidi El Barrak foundation soil, at about 10 m depth, has been achieved in equilateral triangular zone of spacing 2.94 m (fig. 4). Fig. 5 shows the location of zones where vibrocompaction took place.

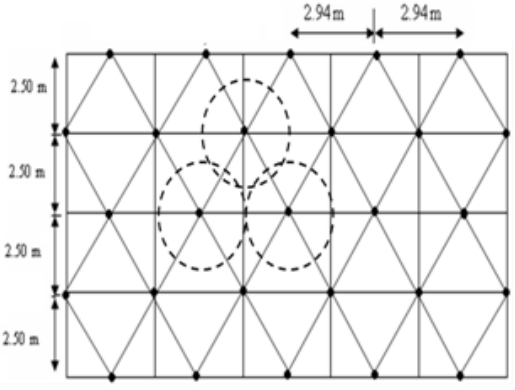

Fig.4 Triangular mesh for the vibrocompaction technique

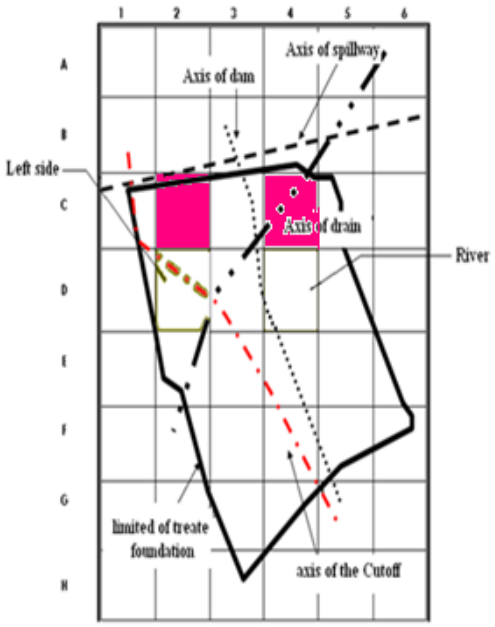

Fig. 5 Vibrocompacted zone

3. CPT-BASED LIQUEFACTION POTENTIAL ANALYSIS OF SIDI EL BARRAK DAM FOUNDATION

As noted previously, the area beneath the Sidi El Barrak dam had been the subject of soil densification using the vibrocompaction technique. A strict quality control program pursued in the project (before and after vibrocompaction) has implemented the CPT test in some locations in the foundation. The zones C2 and C4 were selected as examples of boreholes that presented in situ data to assess the liquefaction potential of the dam foundation.

Zhou (1980) (in Seed et al, 1983) had considered the critical resistance q_{crit} under which liquefaction risk is potential. In fact, they identified the liquefaction potential with the formula:

$$q_{crit} = q_{co}[(1-0{,}065(z_w-2)][1-0{,}05(z_s-2)] \quad (1)$$

Where q_{crit} is the critical resistance for liquefaction potential; q_{c0} is the static penetration resistance that depends on epicentral intensity of considered earthquake; Z_w is the depth of water table level from ground surface (in meters); Z_s is the distance between water table level and point of measurement (in meters).

The CPT data collected before and after the soil improvement of the case study (in the mesh C2) and the threshold curves given by Zhou (1980) for different earthquake intensities are illustrated in figs. 7 and 8.

Before vibrocompaction, the measured values of qc are generally lower than the critical resistance values q_{crit}, showing vulnerability of the dam foundation to liquefaction. The q_c values in the compacted sand increase significantly due to the soil consolidation and rearrangement of particles after soil densification.

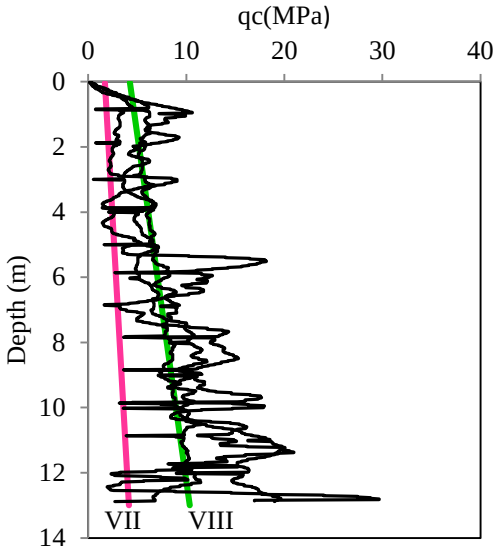

Fig. 7 CPT data before vibrocompaction in C2

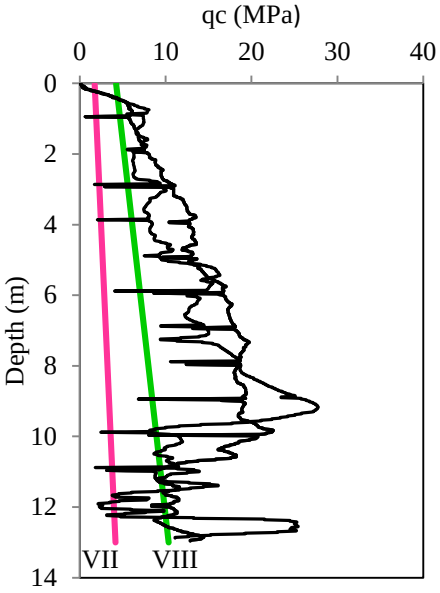

Fig. 8 CPT data after vibrocompaction in C2

Seed and Idriss (1971) outlined a simplified procedure to evaluate the liquefaction resistance of sandy soils using the relative density and the shear stresses induced by earthquake loading. In a later up date, using liquefaction case histories, Seed et

al (1985) proposed a boundary curve which separates sites where liquefaction effects were or were not observed due to an earthquake magnitude of 7.5.

This approach requires an estimate of the seismic demand placed on a soil layer, expressed in term of Cyclic Stress Ratio (CSR) (Youd et al., 1997). They formulated the simplified equation to calculate the CSR as following:

$$CSR = 0.65 \frac{a_{max}}{g} \frac{\sigma_v}{\sigma_v'} r_d \quad (2)$$

Where, σ_v and σ'_v are total and effective vertical overburden stresses, respectively, a_{max} is the peak horizontal acceleration at ground surface generated by the design earthquake. For the case study, a_{max} is equal to 0.2g, g is the acceleration of gravity and r_d is a stress reduction coefficient.

Robertson & Wride (1998) suggested that the boundary curve or CRR can be estimated as a function of the equivalent clean sand normalized penetration resistance (qc1N)cs. Figures 9 and 10 show calculated CSR plotted as a function of the corrected and normalized resistance qc1N from Sidi El Barrak site (in meshes C2 and C4). The pre-treatment data points (solid circles) are plotted below the boundary curve which indicates that the soils in zone C2 and zone C4 are susceptible to the cyclic liquefaction. However, the post-treatment data (open circle) fall above the boundary curve, in the non- liquefaction zone.

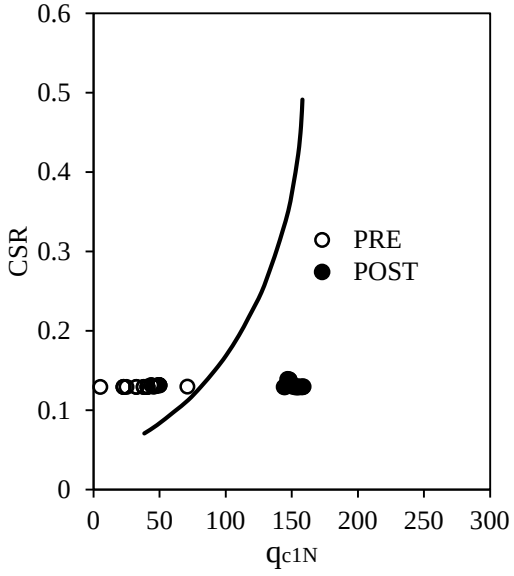

Fig. 9 CSR as a function of q_{c1N} in mesh C2

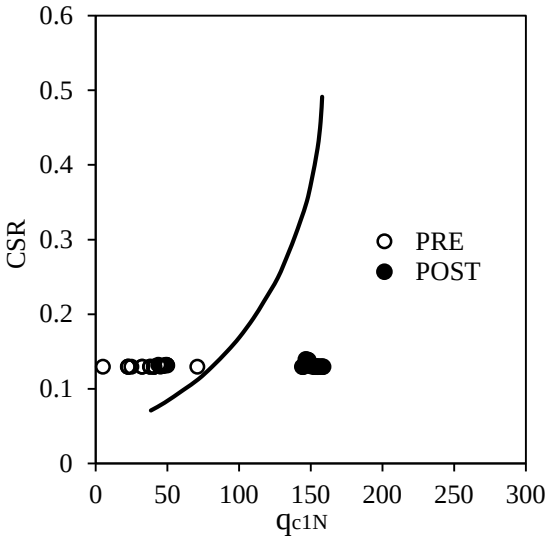

Fig. 10 CSR as a function of q_{c1N} in mesh C4

The results of this deterministic approach are usually presented in a factor of safety (F_S). In theory, liquefaction is predicted to occur if $F_S \leq 1$, and no liquefaction is predicted if $F_S > 1$. Fig. 11 and Fig. 12 show the FS profile calculated from the Robertson & Wride approach in zones C2 and C4 before and after soil improvement. The FS profile obtained from the pre-treatment data are smaller than the critical value (FS = 1). So, the dam foundation may be prone to liquefaction during the design earthquake event. Nevertheless, the FS values of the compacted layers exceed 1. Hence, the soil is not susceptible to liquefaction due to the densification by vibrocompaction.

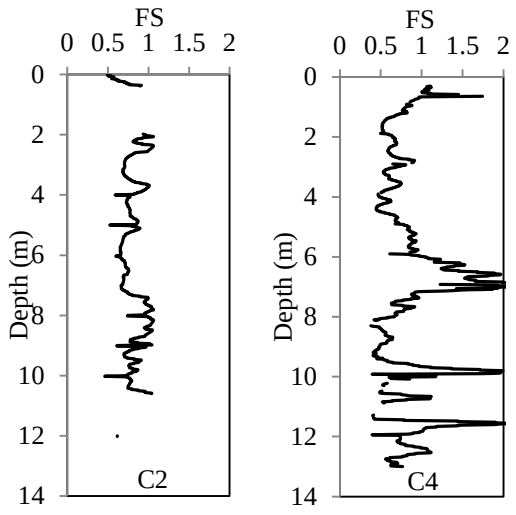

Fig. 11 Fs profile in meshes C2 and C4 before vibrocompaction

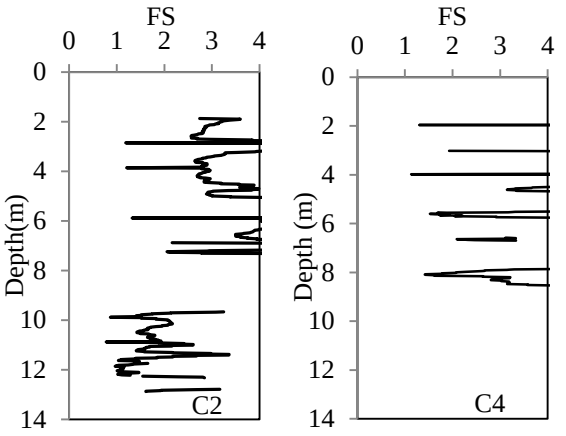

Fig. 12 FS profile in meshes C2 and C4 after vibrocompaction

The deterministic liquefaction evaluation method can only answer whether the soils liquefy (FS ≥ 1) or not (FS < 1). Thus, the probabilistic approach is increasingly used for quantifying the liquefaction hazard of the various verticals and for drawing up liquefaction potential maps. Actually, researchers suggested that any deterministic method must be calibrated so that the meaning of the calculated FS is understood in terms of likelihood or probability of liquefaction. For example, based on both logistic regression and Bayesian mapping approaches, the Robertson method has been calibrated by Juang and Jiang (2000) and the probability of liquefaction PL was presented in the following mapping function:

$$PL = \frac{1}{1+\left(\frac{FS}{A}\right)^{B}} \quad (3)$$

Where PL is the probability of liquefaction and the coefficients A and B are equal to 1.0 and 3.3 respectively.

After Chen and Juang (2000) the likelihood of liquefaction can be interpreted using the calculated probability of liquefaction PL values in Table 1.

Table1 Classification of liquefaction probability

Probability	Likelihood of liquefaction
0.85≤ PL<1	Almost certain that will be liquefy
0.65≤ PL<0.85	Very likely
0.35≤ PL<0.65	Liquefaction/ non liquefaction is equally likely
0.15≤ PL<0.35	Unlikely
0.00≤ PL<0.15	Almost certain will not liquefy

CPT data at the meshes C2 and C4 of the dam foundation are used as example to represent the profiles of the probability of liquefaction PL obtained from the Robertson method (figs. 13-14). Before vibrocompaction (fig. 13), the profiles suggest that the calculated probabilities are high, ranging from 0.4 to 1. The average of probabilities of liquefaction values is about 68%. This value falls into the class of "very likely" in the Juang and Chen classification given in table 1. After vibrocompaction (fig. 14), the average of the calculated probability of liquefaction drops below 35%, indicating a low likelihood of liquefaction of the dam foundation.

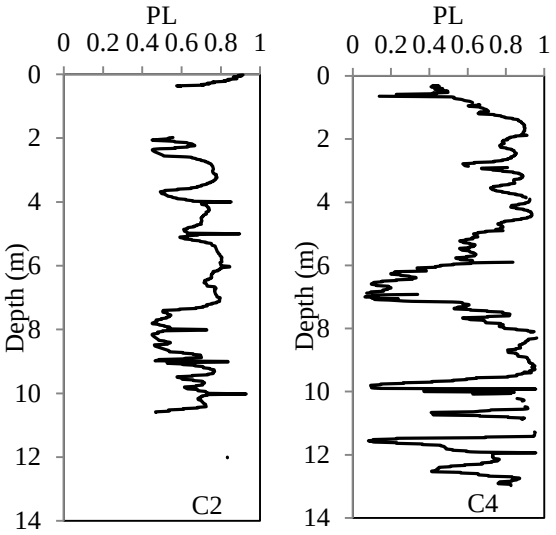

Fig. 13 Profile of P_L from Robertson methods in meshes C2 and C4before vibrocompaction

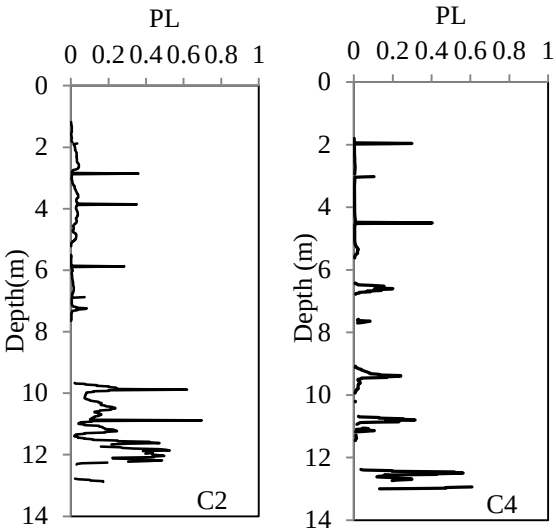

Fig. 14 Profile of P_L from Robertson methods in meshes C2 and C4 after vibrocompaction

Additionally, a probabilistic methodology, based on the use of the liquefied potential index I_L, was applied in order to evaluate the liquefaction hazard of the various explored verticals. The LPI was originally developed by Iwasaki et al (1982) to estimate liquefaction potential causing foundation damage (Holzer et al, 2003). Iwasaki et al (1982) introduce the following form for the liquefaction potential index as given by the equation (10)

$$I_L = \int_0^{20} Fw(z)dz \qquad (4)$$

Based on cases studied in Japan, Iwasaki et al (1982) provided the following liquefaction risk criteria, referred to herein as the Iwasaki criteria:
$I_L = 0$, the liquefaction failure is extremely low;
$0 < I_L \leq 5$, the liquefaction failure is low;
$5 < I_L \leq 10$, the liquefaction failure is high;
$I_L > 15$, the liquefaction failure is extremely high;

In the present study, the Liquefaction Potential Index I_L values were computed using the FS profiles obtained from the Robertson & Wride (1998) method. Then, to identify the liquefaction hazard level in the dam foundation, the Liquefaction Potential Index values were grouped and cumulative distributions of I_L were established.

Figure 15 illustrates the distribution of the calculated I_L values of 20 CPTs sounding using the Robertson method. The results show that only 4% of the untreated points have an I_L less than 5 and 91% of the treated points have an I_L greater than 15. So, according to Iwasaki classification criteria, the liquefaction failure is extremely high in the site of Sidi El Barrak dam. However, after vibrocompaction, it can be observed that 91% of the compacted points have an I_L smaller than 5 which indicate that the liquefaction risk is low.

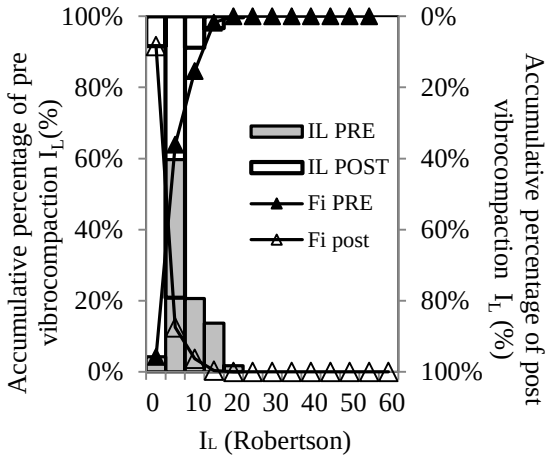

Fig. 15 Distribution of Calculated I_L Values obtained from Robertson method

The increased field performance data have become available at liquefaction sites investigated with CPT tests. These data have facilitated the development of CPT-based liquefaction resistance correlations. Indeed, the CRR relationship derived from the liquefaction correlations by Idriss & Boulanger (2008) is illustrated by the following equation:

$$CRR_{M=7,5} = \exp\left(\frac{q_{c1NCS}}{540} + \left(\frac{q_{c1NCS}}{67}\right)^2 - \left(\frac{q_{c1NCS}}{80}\right)^3 + \left(\frac{q_{c1NCS}}{114}\right)^4 - 3\right) \qquad (5)$$

Where q_{c1NCS} is the fines content corrected penetration resistance.

Figures 16 and 17 represent the Boulanger & Idriss (2008) boundary curve between liquefaction and non liquefaction in C2 and C4 zones. The cyclic stress ratio is plotted as a function of the normalized cone resistance. From these figures, the CPT borings data are plotted below the threshold curve and it is so concluded that liquefaction would occur for untreated soils. After vibrocompaction, the normalized cone resistance increase and the CPT data has exceeded the threshold curve and are not expected to liquefy.

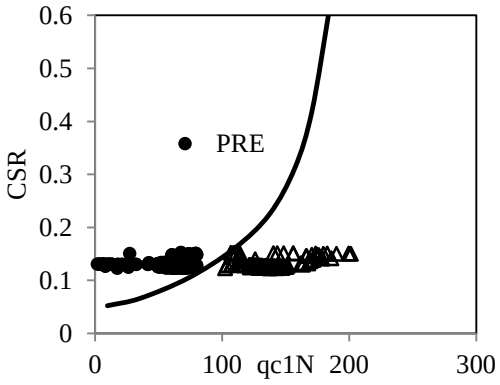

Fig. 16 CSR as a function of q_{c1N} in mesh C2

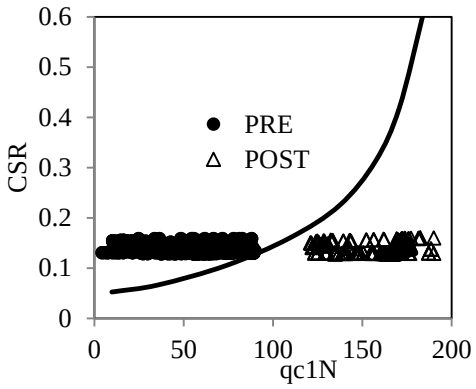

Fig. 17 CSR as a function of q_{c1N} in mesh C4

In the study case, the results of the liquefaction analysis before and after soil compaction, expressed as the profile of safety obtained from the Boulanger & Idriss (2008) correlation, are reported respectively in Fig. 18 and Fig. 19. Before improvement conditions, Fig. 27 shows that the factor of safety appear below the unit value which indicates the investigated layers in zone C2 are susceptible to liquefaction at the expected future earthquake. In Fig. 28, after improvement, the FS values are mostly greater than 1. Thus, the improvement process was effective in eliminating liquefaction potential of the saturated sandy layers.

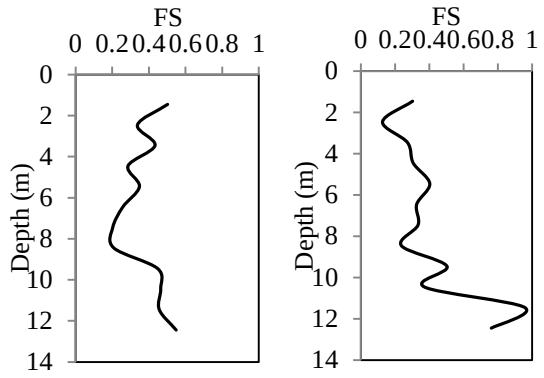

Fig.18 FS profile obtained before vibrocompaction respectively in meshes C2and C4

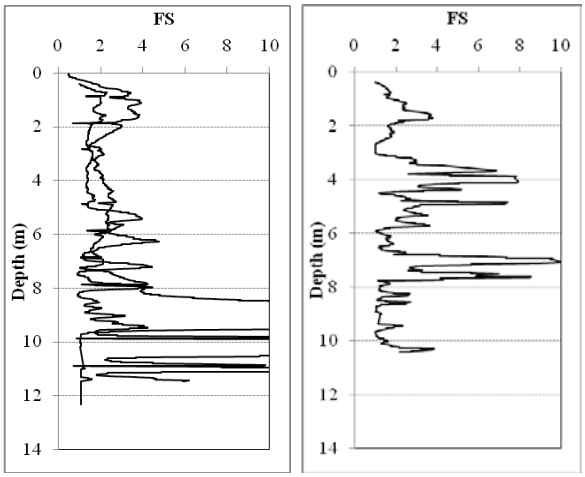

Fig.19 FS profile obtained after vibrocompaction respectively in meshes C2and C4

4. TRIAXIAL TEST RESULTS AT LOW STRAIN AMPLITUDE

In order to evaluate the influence of soil properties on wave propagation during earthquake and their effects on soil-structure interaction, it is essential to know the cyclic behavior of soils for induced strain levels. For this purpose we have developed a modified triaxial apparatus which gave the possibility to measure the cyclic properties of soils within a large range of strain amplitude**.**

4.1 Determination of The Young Modulus

Figure 20 shows the relationship between the Young modulus and cyclic deformation. It is noted that the Young modulus is firstly constant. Then, it decreases with the increase of the amplitude of cyclic deformation. It is clear that the maximum Young modulus increases with the increase of the effective confining stress.

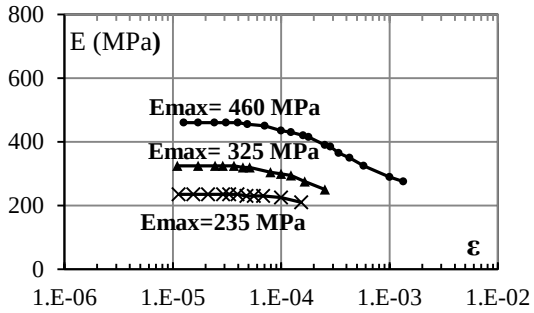

Fig. 20 Variation of Young's Modulus with cyclic strain

4.2 Determination Of The Poisson Ratio

The figure 21 presents an example of the relation between the Poisson's ratio and the axial strain. It is concluded that the Poisson ratio is constant and it decreases with the increase of the isotropic stress.

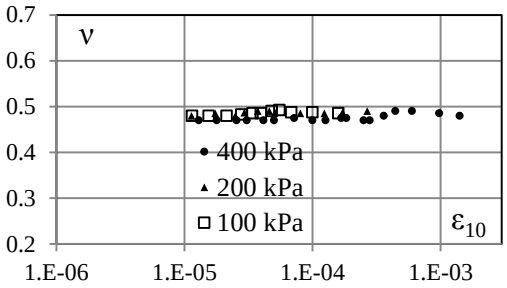

Fig. 21 Variation of Poisson ratio with cyclic strain

5. CONCLUSION

The detailed geotechnical investigation including CPT tests were used effectively to identify the liquefaction potential of the foundation of Sidi El

Barrak dam. The case study demonstrates the successful mitigation of the liquefaction risk under the design earthquake. The factor of safety against liquefaction is obtained from three CPT-based simplified procedures. The results show that the undensified soil layers of foundation were vulnerable to liquefaction hazard (FS < 1). However, after vibrocompaction, the dam foundation was not prone to liquefaction (FS > 1). A comparison shows general agreement between the in situ and laboratory test results.

6. REFERENCES

[1] Zhou S. Evaluation of the liquefaction of sand by static cone penetration test. Proceedings, 7th world conference on earthquake, 1980.

[2] Seed B., Idriss IM., Arango I.,. "Evaluation of liquefaction potential using field performance data". Journal Geotechnical Engineering. ASCE, vol 109, 1983, pp 458-482.

[3] Seed B., Idriss IM.,. "Simplified procedures for evaluating soil liquefaction potential". PROC.JSME, ASCE, Vol 97, 1971, pp. 1249-1273.

[4] Seed H.B., Tokimatsu K., Harder L.F.,Chung RM,. "The influence of SPT Procedures in soil liquefaction". Journal of Geotechnical Engineering, ASCE, Vol. 111, 1985, pp. 1425-1445.

[5] Youd TL., Andrus M., Idriss M.. "Proceedings of the NCEER workshop on evaluation of liquefaction resistance of soils", 1997, pp.1-40.

[6] Robertson PK., Wride C. Evaluating cyclic liquefaction potential using the cone penetration test. Canadian Geotechnical Journal, 1998, pp. 442-459.

[7] Juang C.H., Chen C.J. A rational method for development of limit state for liquefaction evaluation based on shear wave velocity, International Journal for numerical and analytical methods in geomechanics, 2000, pp. 1-24.

[8] Juang C.H., Andrus R., Chen J. Risk- based liquefaction potential evaluation using Standard Penetration Test, Canadian Geotechnical Journal, 2000, pp. 1195-1208.

[9] Holzer T., Toprak S., Bennett M. Application of the liquefaction potential index to liquefaction hazard mapping, in Procceding from the 8th US - Japan workshop on Earthquake resistant design of Lifeline facilities and counterness against liquefaction, 2003.

[10] Boulanger R.W., Idriss I.M. Soil liquefaction during earthquake. California:EERI, 2008, chapiter 1.

Int. J. of GEOMATE, June, 2014, Vol. 6, No. 2 (Sl. No. 12), pp. 919-926.

MS No. 3195 received on June 16, 2013 and reviewed under GEOMATE publication policies.

Corresponding Author: Guettaya Ikram